

Weierstraß-Institut
für Angewandte Analysis und Stochastik
Leibniz-Institut im Forschungsverbund Berlin e. V.

Preprint

ISSN 2198-5855

**New insights on the interfacial tension of electrochemical
interfaces and the Lippmann equation**

Wolfgang Dreyer, Clemens Gohlke, Manuel Landstorfer, Rüdiger Müller

submitted: December 21, 2015

Weierstrass-Institute
Mohrenstr. 39
10117 Berlin
Germany
E-Mail: Wolfgang.Dreyer@wias-berlin.de
Clemens.Gohlke@wias-berlin.de
Manuel.Landstorfer@wias-berlin.de
Ruediger.Mueller@wias-berlin.de

No. 2201
Berlin 2015



2010 *Mathematics Subject Classification.* 78A57 35Q70 35C20.

Key words and phrases. Lippmann equation, Electrochemistry, liquid-liquid interface, asymptotic analysis.

Edited by
Weierstraß-Institut für Angewandte Analysis und Stochastik (WIAS)
Leibniz-Institut im Forschungsverbund Berlin e. V.
Mohrenstraße 39
10117 Berlin
Germany

Fax: +49 30 20372-303
E-Mail: preprint@wias-berlin.de
World Wide Web: <http://www.wias-berlin.de/>

Abstract

The Lippmann equation is considered as universal relationship between interfacial tension, double layer charge, and cell potential. Based on the framework of continuum thermo-electrodynamics we provide some crucial new insights to this relation.

In a previous work we have derived a general thermodynamic consistent model for electrochemical interfaces, which showed a remarkable agreement to single crystal experimental data. Here we apply the model to a curved liquid metal electrode. If the electrode radius is large compared to the Debye length, we apply asymptotic analysis methods and obtain the Lippmann equation. We give precise definitions of the involved quantities and show that the interfacial tension of the Lippmann equation is composed of the surface tension of our general model, and contributions arising from the adjacent space charge layers.

This finding is confirmed by a comparison of our model to experimental data of several mercury-electrolyte interfaces. We obtain qualitative and quantitative agreement in the 2V potential range for various salt concentrations.

We also discuss the validity of our asymptotic model when the electrode radius is comparable to the Debye length.

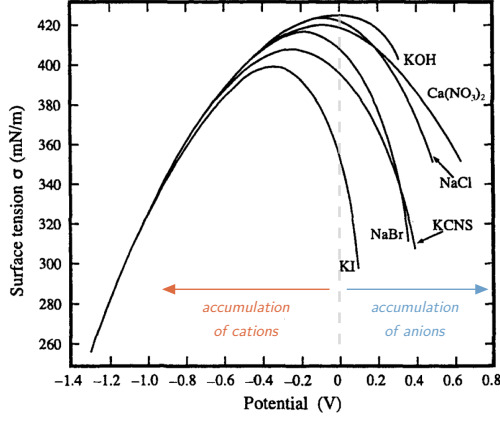
1 Introduction

The interfacial phenomena of electrocapillarity, discovered by Lippmann a century ago[Lip75, Lip73], is a key feature for investigations of the electrochemical double layer which forms at the interface between two charged phases. Intensive experimental studies on mercury-aqueous electrolyte interfaces carried out by Gouy [Gou03, Gou06a, Gou06b, Gou10] Frumkin [Fru28], Grahame [Gra47], and others, lead to fundamental perceptions of the double layer. Experimentally well and reproducibly observed is the parabola shaped relationship between the *interfacial tension* γ and some applied voltage U . However, there are some electrolyte specific deviations in this relationship, which are yet only partly understood. The fundamental thermodynamic basis for this effect is the Lippmann equation[BF01, BRGA02, NTA04], which states

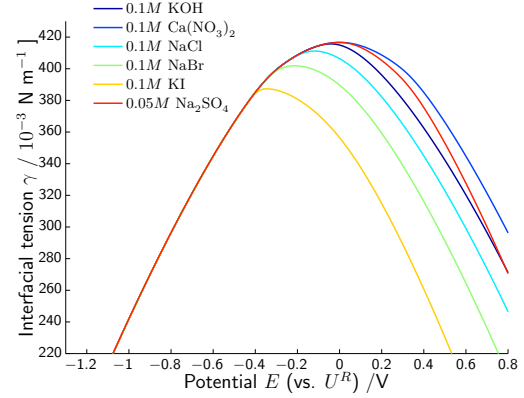
$$\frac{d}{dU}\gamma = Q, \quad (1)$$

where U is the potential difference between metal and electrolyte, γ is interfacial tension, Q is the double layer charge. This relation is widely recognized as a thermodynamic postulation, which is, however, not tenable. Despite, a sharp definition of the quantities in (1) is not as obvious as it might seem.

In this work we derive fundamental relations for interface between two adjacent, charged phases based on continuum thermo-electrodynamics. We obtain general results, e.g. generalizations of



(a) Electrocapillarity curves for various salts according to Fig. 1 from [Gra47] (reprinted with permission)



(b) Computed interfacial tension based on our model.

Figure 1: Comparison between measured data of electrocapillarity curves and computations based on our model.

the Young–Laplace equation for electrochemical interfaces, which are independent of the actual material but rely exclusively on thermodynamic equilibrium assumptions and matched asymptotic methods,

$$p^+ - p^- = 2k_M \gamma. \quad (2)$$

It turns out that the measurable interfacial tension γ actually consists of three contributions, i.e. the surface tension γ_s of the material surface S , and two boundary layer contributions $\tilde{\gamma}^\pm$ of the respective phase. These contributions are structurally very different since they arise from different thermodynamic theories, i.e. volume and surface thermodynamics. But knowledge of this structural decomposition is crucial for a model based understanding of electrochemical interfaces, and we derive the relation (1) with a detailed knowledge on γ and Q within this work.

For a liquid metal-electrolyte interface we obtain further explicit representations of the interfacial contributions based on material functions for the respective phases. For example, we obtain for the electrolytic boundary layer contribution the representation

$$\tilde{\gamma}^E = \int_0^{U^E} \sqrt{2\varepsilon_0(1 + \chi)(p_S^+ - p^E)} dU' \quad (3)$$

where p_S^+ denotes the material pressure right at the interface, while p^E denotes the bulk pressure. This finding fits well to our recently derived model [DGL16, DGL14] of the double layer, where the material pressure p is the crucial ingredient. Additionally, adsorbates contribute to the surface tension γ_s with constituent specific properties, i.e. the corresponding adsorption energy, which explains the deviations in Fig. 1 for the various salts.

For several Hg/aqueous electrolyte solutions we provide numerical computations of the interfacial tension based on our model and compare them to experimental data. Fig. 1 shows results of our

model in comparison to the prominent measurements by Gouy and Grahame []. It is to emphasize that our model allows thus for a quantitative and qualitative model based understanding of electrocapillarity curves. In section 7 we discuss in detail several aspects of our model which lead to the corresponding parameters used to predict the electrocapillarity curves in Fig. 1.

Motivation. We consider a liquid metal in contact with a liquid electrolyte. When a potential is applied, in general a double layer forms at the interface S . In thermodynamic equilibrium the electric field and the stress in the double layer is described by the coupled system of Poisson equation and the momentum balance

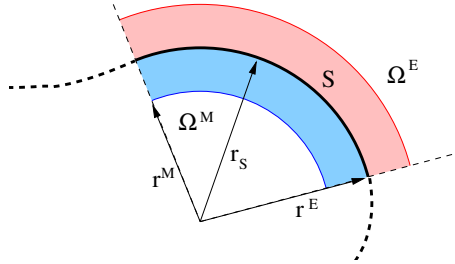
$$\operatorname{div}((1 + \chi)\varepsilon_0 \mathbf{E}) = n^F \quad \llbracket (1 + \chi)\varepsilon_0 \mathbf{E} \cdot \boldsymbol{\nu} \rrbracket = n_s^F \quad (4)$$

$$\operatorname{div}(\boldsymbol{\Sigma}) = 0 \quad \llbracket \boldsymbol{\Sigma} \cdot \boldsymbol{\nu} \rrbracket = -2k_M \gamma \boldsymbol{\nu} - \nabla_s \gamma. \quad (5)$$

Here \mathbf{E} denotes the electric field, χ is the electric susceptibility, γ is the surface tension, and $\boldsymbol{\Sigma}$ is the total stress tensor, which is given by

$$\boldsymbol{\Sigma} = -p\mathbf{1} + (1 + \chi)\varepsilon_0 \left(\mathbf{E} \otimes \mathbf{E} - \frac{1}{2}|\mathbf{E}|^2 \mathbf{1} \right). \quad (6)$$

The contribution of the electric field to the total stress is called the Maxwell stress. The double bracket denotes the jump, i.e. difference, of the bulk quantities at the interface.



Let us assume locally spherical symmetry. Using spherical coordinates (r, θ, ψ) with basis vectors $(\mathbf{e}_r, \mathbf{e}_\theta, \mathbf{e}_\psi)$ the surface S is positioned at r_S and $\mathbf{E} = E_r \mathbf{e}_r$. The total stress tensor reduces to

$$\boldsymbol{\Sigma} = \Sigma_{rr} \mathbf{e}_r \otimes \mathbf{e}_r + \Sigma_{\theta\theta} \mathbf{e}_\theta \otimes \mathbf{e}_\theta + \Sigma_{\psi\psi} \mathbf{e}_\psi \otimes \mathbf{e}_\psi \quad (7)$$

with

$$\Sigma_{rr} = -p + \frac{1+\chi}{2}\varepsilon E_r^2, \quad \Sigma_{\theta\theta} = \Sigma_{\psi\psi} = -p - \frac{1+\chi}{2}\varepsilon E_r^2. \quad (8)$$

The Poisson-momentum equation system reduce to

$$\partial_r(r^2(1 + \chi)\varepsilon_0 E_r) = r^2 n^F, \quad \llbracket (1 + \chi)\varepsilon_0 E_r \rrbracket = n_s^F, \quad (9)$$

$$\partial_r \Sigma_{rr} = -\frac{2}{r}(1 + \chi)\varepsilon_0 E_r^2, \quad \llbracket \Sigma_{rr} \rrbracket = -\frac{2}{r_S} \gamma. \quad (10)$$

Let $r^E > r_S$ a point in the electrolyte and $r^M < r_S$ a point in the metal. Both points are sufficiently far away from the interface. Further we assume that the mean curvature $k_M = -1/r_S$

holds $|k_M r| \approx 1$ for $r \in (r^M, r^E)$. Then we can integrate the bulk equations (9)₁ and (10)₁ with respect to r ,

$$-(1 + \chi)\varepsilon_0(E_r|_{r_S}^{M/E} - E_r|_{r^{M/E}}) = \pm \tilde{q}^{M/E}, \quad (11)$$

$$\Sigma_{rr}|_{r_S}^{M/E} - \Sigma_{rr}|_{r^{M/E}} = \pm 2k_M \tilde{\gamma}^{M/E}. \quad (12)$$

The new quantities are defined as

$$\tilde{q}^{M/E} = \pm \int_{r_S}^{r^{M/E}} n^F dr, \quad \tilde{\gamma}^{M/E} = \pm \int_{r_S}^{r^{M/E}} (1 + \chi)\varepsilon_0 E_r^2 dr. \quad (13)$$

We denote the new quantities as *boundary layer charge* and *boundary layer tension* in the metal and in the electrolyte phase.

The electric field vanishes few nanometers away from the interface. Hence, we can assume $E_r|_{r^{M/E}} = 0$ and therefore $\Sigma_{rr}|_{r^{M/E}} = -p|_{r^{M/E}}$. We obtain from the Poisson-momentum system (9)–(10)

$$0 = n_s^F + \tilde{q}_s^E + \tilde{q}_s^M, \quad (14)$$

$$p|_{r^E} - p|_{r^M} = 2k_M \left(\gamma_s + \tilde{\gamma}_s^M + \tilde{\gamma}_s^E \right). \quad (15)$$

Equation (14) is the electroneutrality condition of the electrical double layer. The second result (15) is quite remarkable. It states that the pressure across the entire electrical double layer is not only dependent on the thermodynamic surface tension γ , but also on the boundary layer tension generated by electric field in the space charge layers. It seems thus appropriate to call

$$\gamma := \gamma_s + \tilde{\gamma}_s^M + \tilde{\gamma}_s^E \quad (16)$$

interfacial tension of the electrical double layer.

The interfacial tension γ serves as the candidate for the Lippmann equation (1). From measurements we know that the charge Q in the Lippmann equation (1) is the electric charge of the whole double layer. For an ideally polarizable electrode the double layer charge is given by

$$Q = \tilde{q}^E + \sum_{\alpha \in \mathcal{M}^E} z_\alpha e_0 n_\alpha, \quad (17)$$

where \mathcal{M}^E is the set of electrolytic species. The voltage difference U between the electrode and the electrolyte is defined as $U = \varphi|_{r^M} - \varphi|_{r^E}$. We will show in section 3 that the definitions of the interfacial tension, charge and applied voltage approximately satisfy the Lippmann equation (1) as well as the Young-Laplace equation (2) in the limit $\lambda \rightarrow 0$, where λ is a dimensionless parameter that controls the width of the boundary layers.

2 Thermodynamical consistent model for equilibrium state

We do not give a detailed derivation of the model here. Our modeling is based on the framework of non-equilibrium thermodynamics [MR59, dM84, BD14] and its extensions to surfaces and

the connection to electrodynamics [Mül85, Bed86]. A general model containing all relevant ingredients for planar interface is provided in [DGM15], the general case for curved interfaces can be found in [Guh15].

Setup. We consider an interface S dividing a domain $\Omega \subseteq \mathbb{R}^3$ into the subdomains Ω^+ and Ω^- . The normal $\boldsymbol{\nu}$ to the interface S always points from Ω^- to Ω^+ . For quantities defined in Ω^+ or Ω^- there will often be corresponding quantities on S . As a convention the same letters are used for these quantities but the surface variables are indicated by a subscript s .

Jumps at interfaces. We introduce the boundary values and the jump of a generic function $u(x)$ in Ω^\pm at the interface S as

$$u|_S^\pm = \lim_{x \in \Omega^\pm \rightarrow S} u \quad \text{and} \quad \llbracket u \rrbracket = u|_S^+ - u|_S^-. \quad (18)$$

In the case the function u is not defined in either Ω^+ or in Ω^- , we set the corresponding value in (18) to zero.

Constituents. In each of the two domains Ω^+ and Ω^- and on the interface S , we consider a mixture of several constituents. In Ω^\pm we denote the constituents by A_α where α is taken from some index set \mathcal{M}^\pm . For each constituent A_α in one of the subdomains Ω^\pm we assume there is a corresponding constituent present on the surface S , but in addition there may be some constituents that are exclusively present on S . The index set for the constituents on S is denoted by \mathcal{M}_S . A constituent A_α has the (atomic) mass m_α and may be carrier of the charge $z_\alpha e_0$, where z_α is the charge number and e_0 is the elementary charge.

Thermodynamic state. In equilibrium, the thermodynamic state in each point $x \in \Omega^\pm$ is described by the number densities n_α of the constituents, the temperature T and the electric field \boldsymbol{E} . The thermodynamic state of the interface S is characterized by the number densities n_α^s of the interfacial constituents and the interfacial temperature T_s .

In equilibrium the temperature T in both domains is constant and continuous at the interface S , i.e. $T = T|_S^\pm$, hence the temperature can be considered as a parameter here.

In equilibrium the electric field can be expressed in terms of the electrostatic potential by $\boldsymbol{E} = -\nabla\varphi$. We assume that the electrostatic potential is continuous at the interface such that the Maxwell equation $\llbracket \nabla\varphi \times \boldsymbol{\nu} \rrbracket = 0$ is satisfied,

$$\varphi = \varphi|_S^- = \varphi|_S^+. \quad (19)$$

The new quantity φ_s is called the *electrostatic surface potential*.

General constitutive assumptions We assume in each subdomain Ω^\pm a constant susceptibility χ . To cover a wide range of materials we assume the free energy densities in Ω^\pm and on S are of the form

$$\rho\psi = \rho\hat{\psi}(T, n_0, \dots, n_N) - \chi \frac{\varepsilon_0}{2} |\nabla\varphi|^2, \quad \rho\psi_s = \rho\hat{\psi}_s(T_s, n_{0s}, \dots, n_{N_s}). \quad (20)$$

The chemical potentials are then defined by

$$\mu_\alpha = \frac{\partial \rho\hat{\psi}}{\partial n_\alpha}, \quad \mu_{\alpha s} = \frac{\partial \rho\hat{\psi}_s}{\partial n_{\alpha s}}. \quad (21)$$

By means of the Gibbs-Duhem relation we introduce the material pressure and the surface tension

$$p = -\rho\hat{\psi} + \sum_{\alpha=0}^N n_\alpha \mu_\alpha, \quad \gamma_s = \rho\hat{\psi}_s - \sum_{\alpha=0}^{N_s} n_{\alpha s} \mu_{\alpha s}. \quad (22)$$

Model equations and boundary conditions In equilibrium, the mass balances, momentum balance and Maxwell's equations in Ω^\pm reduce to [DGM15, DGL16]

$$\nabla(\mu_\alpha + z_\alpha e_0 \varphi) = \mathbf{b} \quad \text{for } \alpha \in \mathcal{M}^\pm, \quad (23a)$$

$$-(1 + \chi)\varepsilon_0 \Delta\varphi = n^F. \quad (23b)$$

A direct calculation shows that the momentum balance results from the equation system above and the Gibbs-Duhem relation (22)_{left}

$$-\operatorname{div}(\boldsymbol{\Sigma}) = \rho\mathbf{b}, \quad (23c)$$

where $\rho\mathbf{b}$ is the force densities due to gravitation and $\boldsymbol{\Sigma}$ is the total stress tensor,

$$\boldsymbol{\Sigma} = -p\mathbf{1} + (1 + \chi)\varepsilon_0(\nabla\varphi \otimes \nabla\varphi - \tfrac{1}{2}|\nabla\varphi|^2\mathbf{1}). \quad (23d)$$

The boundary conditions at S , which follow from surface balance equations, are [Mül85, Guh15]

$$\mu_\alpha|_S^\pm = \mu_{\alpha s} \quad \text{for } \alpha \in \mathcal{M}^\pm, \quad (24a)$$

$$-[\boldsymbol{\Sigma} \cdot \boldsymbol{\nu}] = 2k_M \gamma_s \boldsymbol{\nu} + \rho\mathbf{b}_s + \nabla_s \gamma, \quad (24b)$$

$$[\nabla\varphi \cdot \boldsymbol{\nu}] = n_s^F. \quad (24c)$$

3 Reduced models for bulk and boundary layers

To derive a general Lippmann equation based on the rigorous thermodynamic model we need to consider asymptotic limit of thin double layers, that can be described by the reduced models summarized below.

When two electrochemical systems are brought into contact it is well-known that narrow boundary layer are formed adjacent to the contact surface. The width of the layers is in the order of the Debye-length which for liquid electrolytes is usually in the range of nanometers. If the macroscopic size L^{ref} of the system is in the range of centimeters, one can introduce a small dimensionless number λ to represent the Debye length as λL^{ref} . Since the solution of the above model (23)-(24) depends on the relation between these different length scales, we add from now on an upper index λ to all the functions.

3.1 Formal asymptotic analysis

We use the method of formal asymptotic analysis to derive a reduced model for a planar interface in non-equilibrium. We refer to [DGM15] for a detailed description of the method. The basic concept of the method is described below.

Let u^λ be a generic function from our list of state variables in Ω^\pm . We assume $\lambda \ll 1$ and approximate u^λ in the bulk by an *outer expansion* with respect to the small parameter

$$u^\lambda = u^{(0)} + \lambda u^{(1)} + \lambda^2 u^{(2)} + \dots \quad (25)$$

where the newly introduced functions $u^{(0)}, u^{(1)}, u^{(2)}, \dots$ still need to be determined. For a function F of u^λ the expansion is given by a Taylor series

$$F(u^\lambda) = F(u^{(0)}) + \lambda F'(u^{(0)})u^{(1)} + \mathcal{O}(\lambda^2). \quad (26)$$

We use the abbreviations $F^{(0)} = F(u^{(0)})$ and $F^{(1)} = F'(u^{(0)})u^{(1)}$ for the leading and higher order terms. In analogous way we introduce expansions of the state variables on surface and for functions thereof.

If $\lambda \ll 1$, the boundary layer constitutes only a small portion of the domains Ω^\pm and the outer expansion does not necessarily have to be accurate inside the layers. Therefore we introduce an additional *inner expansion* inside the layer, which is based on space coordinates that are rescaled by λ in the normal direction. To distinguish between the two expansions in the bulk and in the boundary layer, we denote the inner expansion by \tilde{u}^λ and write

$$\tilde{u}^\lambda = \tilde{u}^{(0)} + \lambda \tilde{u}^{(1)} + \lambda^2 \tilde{u}^{(2)} + \dots \quad (27)$$

The two approximations have to be related by so called matching conditions which are detailed in Sect. 4.4 below. While the variables in the inner expansion have to satisfy the boundary conditions at S , for the outer expansion the role of the boundary conditions is taken by the matching conditions. Nevertheless, a definition of boundary values and jumps analogous to (18) can also be made for the variables of the outer expansion in the bulk, but we prefer to apply a different notation here to highlight the interpretation as jumps over the complete double layer. We denote the leading order parameterization of the interface S by I and define for a generic function $u^{(0)}$ on the regions Ω^\pm

$$u^{(0)}|_I^\pm = \lim_{x \rightarrow I^\pm} u^{(0)} \quad \text{and} \quad \llbracket u^{(0)} \rrbracket = u^{(0)}|_I^+ - u^{(0)}|_I^-. \quad (28)$$

An equivalent definition holds for the higher order $u^{(1)}$. By the formal asymptotic analysis carried out in Sect. 4 it is possible to derive model equations for the variables of the inner and the outer expansions with boundary conditions for the bulk variables that incorporate all double layer information in a consistent way. Here we summarize the results.

3.2 Constant leading order bulk quantities

The general constitutive assumptions are analogous to (20)–(22) above. In leading order the free energy density simplifies to

$$\rho\psi^{(0)} = \rho\hat{\psi}^{(0)}(T, n_0^{(0)}, \dots, n_N^{(0)}) . \quad (29)$$

In each of the subdomains Ω^\pm we have constant number densities $n_\alpha^{(0),\pm}$ and a constant electrostatic potential $\varphi^{(0),\pm}$. Hence, there is a well defined electric potential difference over the interface I . For species which are defined in both domains Ω^+ and Ω^- the electrochemical potential is continuous at I , i.e.

$$\llbracket \mu_\alpha^{(0)} + z_\alpha e_0 \varphi^{(0)} \rrbracket = 0 \quad \text{at } I \quad \text{for } \alpha \in \mathcal{M}^+ \cap \mathcal{M}^- . \quad (30)$$

Moreover, the jump condition

$$\llbracket p^{(0)} \rrbracket = 0 \quad \text{at } I \quad (31)$$

implies that in leading order the pressure $p^{(0)}$ is constant in Ω . Thus gravitation and surface tension have to be considered as higher order effects.

3.3 Surface and boundary layer equations of the leading order

Given the input data $\varphi^{(0),\pm}$ and $n_\alpha^{(0),\pm}$ from the leading order problem, we can determine the surface number densities $n_{\alpha s}^{(0)}$ and the surface electrostatic potential $\varphi_s^{(0)}$ as well as $\tilde{\varphi}^{(0)}, \tilde{n}_\alpha^{(0)}$ in the boundary layers.

Surface. The number densities n_α and $\varphi^{(0)}$ are determined by

$$\mu_\alpha^{(0),\pm} + z_\alpha e_0 \varphi^{(0),\pm} = \mu_{\alpha s}^{(0)} + z_\alpha e_0 \varphi_s^{(0)} \quad \text{at } I \quad \text{for } \alpha \in \mathcal{M}^\pm , \quad (32a)$$

$$0 = n_s^{\text{F},(0)} + \tilde{q}^+ + \tilde{q}^- \quad \text{at } I , \quad (32b)$$

where the boundary charges are defined as functions of boundary layer quantities,

$$\tilde{q}^\pm = \pm \int_0^{\pm\infty} \tilde{n}^{\text{F},(0)} dx . \quad (33)$$

Boundary layer. In the boundary layer we only have to solve differential equations in one space dimension which we denote by z , i.e.

$$\partial_z(\tilde{\mu}_\alpha^{(0)} + z_\alpha e_0 \tilde{\varphi}^{(0)}) = 0, \quad \text{for } \alpha \in \mathcal{M}^\pm, \quad (34)$$

$$-(1 + \chi)\varepsilon_0 \partial_{zz} \tilde{\varphi}^{(0)} = \tilde{n}^{F,(0)}, \quad (35)$$

with boundary conditions

$$\lim_{z \rightarrow \pm\infty} \tilde{n}_\alpha^{(0)} = n_\alpha^{(0),\pm}, \quad \text{for } \alpha \in \mathcal{M}^\pm, \quad (36)$$

$$\lim_{z \rightarrow \pm\infty} \tilde{\varphi}^{(0)} = \varphi_s^{(0),\pm}, \quad \text{and} \quad \tilde{\varphi}^{(0)}|_{z=0}^\pm = \varphi_s^{(0)}. \quad (37)$$

We see that $\varphi_s^{(0)}$ is independent of the space coordinates and thus there is a well defined potential difference between the surface and each of the bulk domains Ω^\pm in leading order.

In the boundary layer the momentum balance has the representation

$$\partial_z \tilde{p}^{(0)} + \tilde{n}^{F,(0)} \partial_z \tilde{\varphi}^{(0)} = 0. \quad (38)$$

We define the quantities

$$\tilde{\gamma}^\pm = \pm \int_0^{\pm\infty} (1 + \chi)\varepsilon_0 |\partial_z \tilde{\varphi}^{(0)}|^2 dx \quad (39)$$

as boundary layer tensions. The meaning of this definition becomes accessible in the following section.

3.4 Higher order bulk and surface model

The variables in first order are the electrostatic potential $\varphi^{(1)}$ and the number densities $n_\alpha^{(1)}$. They are related to the chemical potentials as $\mu_\alpha^{(1)} = \sum_\beta (\frac{\partial \mu_\alpha}{\partial n_\beta})^{(0)} n_\beta^{(1)}$. The governing equations in Ω^\pm are

$$\nabla(\mu_\alpha^{(1)} + z_\alpha e_0 \varphi^{(1)}) = \mathbf{b} \quad \text{for } \alpha \in \mathcal{M}^\pm, \quad (40a)$$

$$0 = n^{F,(1)}. \quad (40b)$$

From these equations and the Gibbs-Duhem equation in the first order, the momentum balance follows as

$$\nabla p^{(1)} = \rho^{(0)} \mathbf{b}. \quad (41)$$

Thus, due to gravitation the pressure as well as the electrochemical potentials are not constant in the first higher order.

The boundary conditions at the thin double layer interface I are

$$\llbracket \mu_\alpha^{(1)} + z_\alpha e_0 \varphi^{(1)} \rrbracket = 0 \quad \text{for } \alpha \in \mathcal{M}^+ \cap \mathcal{M}^-, \quad (42a)$$

$$\llbracket p^{(1)} \rrbracket = 2k_M^{(0)} (\gamma_s^{(0)} + \tilde{\gamma}^+ + \tilde{\gamma}^-), \quad (42b)$$

where $\gamma_s^{(0)}$ is the surface tension given by the Gibbs-Duhem equation (22)_{right} in the leading order and the boundary layer tensions $\tilde{\gamma}^\pm$ are defined in (39).

3.5 Lippmann equation

Based on the reduced models of the preceding sections, the Lippmann equation is derived in Sect. (5), here we give a definition of the involved quantities and state the result.

According to (31), the pressure in leading order is continuous across the double layer. Thus the first relevant contributions have to be of higher order. In the first order, the jump of the pressure is given by the Young-Laplace-equation (42b), where the interfacial tension γ of the reduced model is composed of the thermodynamic surface tension $\gamma_s^{(0)}$ and two electromagnetic contributions $\tilde{\gamma}^\pm$, viz.

$$\gamma = \gamma_s^{(0)} + \tilde{\gamma}^+ + \tilde{\gamma}^- . \quad (43)$$

Because the electric potential in Ω^\pm in leading order is independent of the space variable, there is a well defined potential difference

$$U = \varphi^{(0),+} - \varphi^{(0),-} . \quad (44)$$

While the complete double layer is electric neutral, cf. (32b), there is the reasonable definition of the electric charge of the double layer, cf. [DGL16]

$$Q = \sum_{\alpha \in \mathcal{M}^-} z_\alpha e_0 n_\alpha^{(0)} + \tilde{q}^- . \quad (45)$$

In the case where no surface reactions are considered and on the basis of the underlying asymptotic analysis for the derivation of the reduced models, we get with the above definitions the Lippmann-equation

$$\frac{d}{dU} \gamma = Q . \quad (46)$$

4 Derivation of the reduced models

4.1 Summary of model equations in dimensionless form

We introduce scaling constants L^{ref} , n^{ref} and m^{ref} that are related to characteristic length, particle density and molecular weight in the system and introduce a characteristic surface particle density n_s^{ref} on the interface S . The scaling generates the dimensionless numbers

$$\lambda = \sqrt{\frac{\varepsilon_0 k T}{e_0^2 n^{ref} (L^{ref})^2}} , \quad \lambda \delta = \frac{n_s^{ref}}{n^{ref} L^{ref}} . \quad (47)$$

The length λL^{ref} is related to the well known Debye length which controls the width of the boundary layers. Then, the dimensionless version of the model equations reads

$$\nabla(\mu_\alpha + z_\alpha \varphi) = \lambda \mathbf{b} \quad \text{for } \alpha \in \mathcal{M}^\pm , \quad (48a)$$

$$-\lambda^2 (1 + \chi) \Delta \varphi = n^F . \quad (48b)$$

The dimensionless jump conditions on the interface S are represented by

$$(\mu_\alpha + z_\alpha \varphi)|_S^\pm = (\mu_\alpha + z_\alpha \varphi)_s^\pm \quad \text{for } \alpha \in \mathcal{M}^\pm, \quad (49a)$$

$$\llbracket p\boldsymbol{\nu} - (1 + \chi)\lambda^2(\partial_\nu \varphi \nabla \varphi - \tfrac{1}{2}|\partial_\nu \varphi|^2 \boldsymbol{\nu}) \rrbracket = \lambda \delta (2k_M \gamma_s \boldsymbol{\nu} + \lambda \rho_s \mathbf{b}_s + \nabla_s \gamma_s), \quad (49b)$$

$$-\llbracket \lambda(1 + \chi)\partial_\nu \varphi \rrbracket = \delta n_s^F. \quad (49c)$$

Pressure and surface tension are given by

$$p = -\rho\psi + \sum_{\alpha=0}^N n_\alpha \mu_\alpha, \quad \gamma_s = \rho_s \psi_s - \sum_{\alpha=0}^{N_s} n_{\alpha s} \mu_{\alpha s}. \quad (50)$$

and the momentum balance can be recovered from (48a) and (50), i.e.

$$\nabla p + n^F \nabla \varphi = \lambda \rho \mathbf{b}. \quad (51)$$

4.2 Formal asymptotic expansion and bulk equations

Leading order. From (48) we can directly read off the leading order bulk equation in Ω^\pm

$$\nabla(\mu_\alpha^{(0)} + z_\alpha \varphi^{(0)}) = 0 \quad \text{for } \alpha \in \mathcal{M}^\pm, \quad (52a)$$

$$0 = n^{F,(0)}. \quad (52b)$$

As a consequence we see that $\varphi^{(0)}$ and all $n_\alpha^{(0)}$ are constant in each of the subdomains Ω^\pm . Since $n^{F,(0)} = 0$, the momentum balance simplifies to

$$\nabla p^{(0)} = 0 \quad (53)$$

and thus also the pressure is constant in each of the subdomains Ω^\pm .

Higher order. The bulk equations in the order $\mathcal{O}(\lambda)$ are

$$\nabla(\mu_\alpha^{(1)} + z_\alpha \varphi^{(1)}) = \mathbf{b}, \quad (54a)$$

$$0 = n^{F,(1)}. \quad (54b)$$

and the momentum balance in higher order can be recovered as

$$\nabla p^{(1)} = \rho^{(0)} \mathbf{b}. \quad (55)$$

4.3 Expansion of surface and boundary layers

Locally, points on the interface S can be represented as $\mathbf{r}(s_1, s_2)$. The partial derivatives $\partial_1 \mathbf{r}$ and $\partial_2 \mathbf{r}$ define the tangential vectors $\boldsymbol{\tau}_1$ and $\boldsymbol{\tau}_2$, respectively, which we assume to be orthogonal. In a neighborhood \mathcal{U} of a smooth surface S , the distance function is well defined. Each point

$\mathbf{x} \in \mathcal{U}$ has a representation $\mathbf{x} = \mathbf{r} + z\boldsymbol{\nu}$, where z is the distance to S . For a generic variable u defined on \mathcal{U} , we introduce rescaled inner variable \tilde{u} by defining

$$\tilde{u}(s_1, s_2, z) = u(\mathbf{r}(s_1, s_2) + \lambda z\boldsymbol{\nu}) . \quad (56)$$

$$\tilde{u} = \tilde{u}^{(0)} + \lambda \tilde{u}^{(1)} + \mathcal{O}(\lambda^2) . \quad (57)$$

Moreover, we assume that the parameterization and the normal can be expanded as

$$\mathbf{r}(s_1, s_2) = \mathbf{r}^{(0)}(s_1, s_2) + \lambda \mathbf{r}^{(1)}(s_1, s_2) + \mathcal{O}(\lambda^2) , \quad (58a)$$

$$\boldsymbol{\nu}(s_1, s_2) = \boldsymbol{\nu}^{(0)}(s_1, s_2) + \lambda \boldsymbol{\nu}^{(1)}(s_1, s_2) + \mathcal{O}(\lambda^2) , \quad (58b)$$

Transformation of derivatives The rescaling in normal direction leads to the following relations for the derivatives, cf. [DGK14]:

$$\nabla u = \lambda^{-1} \partial_z \tilde{u} \boldsymbol{\nu} + |\boldsymbol{\tau}_1|^{-2} \partial_1 \tilde{u} \boldsymbol{\tau}_1 + |\boldsymbol{\tau}_2|^{-2} \partial_2 \tilde{u} \boldsymbol{\tau}_2 + \mathcal{O}(\lambda) , \quad (59a)$$

$$\operatorname{div}(\mathbf{u}) = \lambda^{-1} \partial_z \tilde{\mathbf{u}} \cdot \boldsymbol{\nu} + \operatorname{div}_{\boldsymbol{\tau}}(\tilde{\mathbf{u}}) + \mathcal{O}(\lambda) , \quad (59b)$$

$$-\Delta u = -\lambda^{-2} \partial_{zz} \tilde{u} - \lambda^{-1} 2k_M \partial_z \tilde{u} + \mathcal{O}(1) , \quad (59c)$$

where $\operatorname{div}_{\boldsymbol{\tau}}$ denotes the surface divergence. If S does not depend on λ , the $\mathcal{O}(\lambda)$ terms in (59a) and (59b) vanish.

Equations in inner variables The model equations in inner variables read

$$(\partial_z \tilde{\mu}_\alpha + z_\alpha \partial_z \tilde{\varphi}) + \mathcal{O}(\lambda^2) = 0 , \quad (60a)$$

$$(\partial_{1,2} \tilde{\mu}_\alpha + z_\alpha \partial_{1,2} \tilde{\varphi}) + \mathcal{O}(\lambda) = 0 , \quad (60b)$$

$$-(1 + \chi)(\partial_{zz} \tilde{\varphi} + \lambda 2k_M \partial_z \tilde{\varphi}) + \mathcal{O}(\lambda^2) = \tilde{n}^F . \quad (60c)$$

The dimensionless jump conditions on the interface S are represented by

$$(\tilde{\mu}_\alpha + z_\alpha \tilde{\varphi})|_S^\pm = (\mu_\alpha + z_\alpha \varphi)|_s \quad (61a)$$

$$\llbracket \tilde{p} - \frac{1+\chi}{2} |\partial_z \tilde{\varphi}|^2 \rrbracket = \lambda \delta 2k_M \gamma + \mathcal{O}(\lambda^2) , \quad (61b)$$

$$-\llbracket (1 + \chi) \partial_z \tilde{\varphi} \partial_{1,2} \tilde{\varphi} \rrbracket = \delta \partial_{1,2} \gamma + \mathcal{O}(\lambda) , \quad (61c)$$

$$-\llbracket \lambda(1 + \chi) \partial_z \tilde{\varphi} \rrbracket = \delta \lambda n_s^F + \mathcal{O}(\lambda^2) . \quad (61d)$$

Also in the layers we can recover the momentum balance from (60) and the Gibbs-Duhem relation

$$(\partial_z \tilde{p} + \tilde{n}^F \partial_z \tilde{\varphi}) + \mathcal{O}(\lambda^2) = 0 , \quad (62)$$

$$(\partial_{1,2} \tilde{p} + \tilde{n}^F \partial_{1,2} \tilde{\varphi}) + \mathcal{O}(\lambda) = 0 , \quad (63)$$

Leading order system. After solving the inner and the outer problem, it turns out that the inner tangential equations (60b), (63) and the surface equations (61c) do not contribute any additional independent information. Thus they are omitted here. The remaining inner equations in leading order read

$$\partial_z(\tilde{\mu}_\alpha^{(0)} + z_\alpha \tilde{\varphi}^{(0)}) = 0, \quad (64a)$$

$$\partial_z \tilde{p}^{(0)} + \tilde{n}^{F,(0)} \partial_z \tilde{\varphi}^{(0)} = 0, \quad (64b)$$

$$-(1 + \chi) \partial_{zz} \tilde{\varphi}^{(0)} = \tilde{n}^{F,(0)}. \quad (64c)$$

In particular, the inner electrochemical potentials are constant in leading order. The jump conditions in leading order are

$$(\tilde{\mu}_\alpha^{(0)} + z_\alpha \tilde{\varphi}^{(0)})|_{z=0}^\pm = \mu_\alpha^{(0)} + z_\alpha \varphi_s^{(0)}, \quad (65a)$$

$$[\tilde{p}^{(0)} - \frac{1+\chi}{2} |\partial_z \tilde{\varphi}^{(0)}|^2] = 0, \quad (65b)$$

$$-[(1 + \chi) \partial_z \tilde{\varphi}^{(0)}] = \delta n_s^{F,(0)}. \quad (65c)$$

Higher order. As in the leading order, the inner tangential equations and the surface equations can be omitted. The remaining first order of the equation system (60) is

$$\partial_z(\tilde{\mu}_\alpha^{(1)} + z_\alpha \tilde{\varphi}^{(1)}) = 0, \quad (66a)$$

$$\partial_z \tilde{p}^{(1)} + \tilde{n}^{F,(0)} \partial_z \tilde{\varphi}^{(1)} + \tilde{n}^{F,(1)} \partial_z \tilde{\varphi}^{(0)} = 0, \quad (66b)$$

$$-(1 + \chi) (\partial_{zz} \tilde{\varphi}^{(1)} + 2k_M \partial_z \tilde{\varphi}^{(0)}) = \tilde{n}^{F,(1)}. \quad (66c)$$

We see that the electrochemical potentials in the layers are also constant in the first order. The higher order jump conditions for the chemical potentials and the pressure are

$$(\tilde{\mu}_\alpha^{(1)} + z_\alpha \tilde{\varphi}^{(1)})|_{z=0}^\pm = (\mu_\alpha^{(1)} + z_\alpha \varphi_s^{(1)}) \quad (67a)$$

$$[\tilde{p}^{(1)} - (1 + \chi) \partial_z \tilde{\varphi}^{(0)} \partial_z \tilde{\varphi}^{(1)}] = \delta 2k_M^{(0)} \gamma_s^{(0)}. \quad (67b)$$

4.4 Matching of inner and outer expansions

Inner and outer expansions are related by so called matching conditions. In [CF88, Peg89] the matching conditions are formally achieved by inserting the corresponding expansions into the left and right hand sides of (58) and subsequent comparison of powers of λ . The result is, cf. [DGK14]:

$$\tilde{u}^{(0)}(z) - u^{(0),\pm}(\mathbf{r}^{(0)}) = o(1/|z|), \quad (68a)$$

$$\partial_z \tilde{u}^{(0)}(z) = o(1/|z|), \quad (68b)$$

and for the terms in higher order we get

$$\tilde{u}^{(1)}(z) - z \partial_\nu u^{(0),\pm}(\mathbf{r}^{(0)}) - u^{(1),\pm}(\mathbf{r}^{(0)}) = o(1/|z|), \quad (69a)$$

$$\partial_z \tilde{u}^{(1)}(z) - \partial_\nu u^{(0),\pm}(\mathbf{r}^{(0)}) = o(1/|z|), \quad (69b)$$

Whenever a variable is constant inside the layer, we get by the matching conditions a relation of the boundary values from the outer expansion to the boundary values of the inner variables at S .

Leading order Since the inner electrochemical potentials are constant according to (64a) the matching conditions can be used to relate the electrochemical potentials of the outer expansion to the boundary values of (65a), viz.

$$\mu_\alpha^{(0)}|_I^\pm + z_\alpha \varphi^{(0)}|_I^\pm = \mu_\alpha^{(0)} + z_\alpha \varphi_s^{(0)}. \quad (70)$$

Using the momentum balance equation (64b) and the Poisson equation (64c) we can rewrite the jump condition (65b) into

$$p^{(0)}|_I^+ = p^{(0)}|_I^-. \quad (71)$$

Higher order bulk We introduce the boundary layer charges and boundary layer tension in the layers as

$$\tilde{q}^\pm = \pm \int_0^{\pm\infty} \tilde{n}^{F,(0)} dx, \quad \tilde{\gamma}^\pm = \pm \int_0^{\pm\infty} (1 + \chi)(\partial_z \tilde{\varphi}^{(0)})^2 dz. \quad (72)$$

Integration of (64c) and the matching condition for $\partial_z \tilde{\varphi}^{(0)}$ show that the jump condition (65c) can be written in the form

$$0 = n_s^{F,(0)} + \tilde{q}^+ + \tilde{q}^-. \quad (73)$$

From Poisson equations (64c) and (66c) at leading and higher order we get

$$\begin{aligned} & \partial_z \tilde{p}^{(1)} + \tilde{n}^{F,(0)} \partial_z \tilde{\varphi}^{(1)} + \tilde{n}^{F,(1)} \partial_z \tilde{\varphi}^{(0)} \\ &= \partial_z \tilde{p}^{(1)} - (1 + \chi) \partial_z (\partial_z \tilde{\varphi}^{(0)} \partial_z \tilde{\varphi}^{(1)}) - 2k_M^{(0)} (1 + \chi) (\partial_z \tilde{\varphi}^{(0)})^2. \end{aligned} \quad (74)$$

Thus the momentum balance (66b) can be rewritten as

$$\partial_z \tilde{p}^{(1)} - (1 + \chi) \partial_z (\partial_z \tilde{\varphi}^{(0)} \partial_z \tilde{\varphi}^{(1)}) = 2k_M^{(0)} (1 + \chi) (\partial_z \tilde{\varphi}^{(0)})^2. \quad (75)$$

Integration from $z = 0$ to $\pm\infty$ yields

$$p^{(1)}|_I^\pm - \left(\partial_z \tilde{p}^{(1)} - (1 + \chi) \partial_z (\partial_z \tilde{\varphi}^{(0)} \partial_z \tilde{\varphi}^{(1)}) \right) \Big|_{z=0}^\pm = \pm 2k_M^{(0)} \tilde{\gamma}^\pm, \quad (76)$$

where we have used the matching conditions (68b)/(69a) and the bulk equation (53). Now, we can write the jump condition (67b) as

$$p^{(1)}|_I^+ - p^{(1)}|_I^- = 2k_M^{(0)} (\gamma_s^{(0)} + \tilde{\gamma}^+ + \tilde{\gamma}^-). \quad (77)$$

Finally, due to the constancy of the inner electrochemical potentials we can relate the electrochemical potentials of the outer expansion to the boundary values at S by

$$\mu_\alpha^{(1)}|_I^\pm + z_\alpha \varphi^{(1)}|_I^\pm = \mu_\alpha^{(1)} + z_\alpha \varphi_s^{(1)}. \quad (78)$$

5 Derivation of the Lippmann equation

For the following derivation it is important to keep in mind, that within the leading order bulk system in Ω^\pm the electric potential is constant $\varphi^{(0),\pm}$ such that there is a well defined potential difference across the interface I

$$U := \varphi^{(0),+} - \varphi^{(0),-} . \quad (79)$$

Moreover, the number densities $n_\alpha^{(0),\pm}$ and hence $\mu_\alpha^{(0),\pm}$ are constant in Ω^\pm and independent of U . Finally, the pressure is constant in Ω and we denote $p^{ref} = p^{(0)}$.

Surface contribution From Gibbs-Duhem and global electroneutrality we infer

$$\begin{aligned} \frac{d}{dU_s} \gamma^{(0)} &= \frac{d}{dU_s} \rho_s^{(0)} \hat{\psi}_s^{(0)} - \sum_{\alpha \in \mathcal{M}_S} \frac{d}{dU_s} (n_s^{(0)} \mu_s^{(0)}) = - \sum_{\alpha \in \mathcal{M}_S} n_s^{(0)} \frac{d}{dU_s} \mu_s^{(0)} \\ &= - \sum_{\alpha \in \mathcal{M}_S} n_s^{(0)} \frac{d}{dU_s} (\mu_s^{(0)} + z_\alpha e_0 \varphi_s^{(0)}) - (\tilde{q}^+ + \tilde{q}^-) \frac{d}{dU_s} \varphi_s^{(0)} \end{aligned} \quad (80)$$

We reformulate the electrochemical potentials in terms of bulk variables as

$$\frac{d}{dU_s} \gamma^{(0)} = - \sum_{\alpha \in \mathcal{M}^\pm} n_s^{(0)} \frac{d}{dU_s} (\mu_\alpha^{(0),\pm} + z_\alpha e_0 \varphi^{(0),\pm}) - (\tilde{q}^+ + \tilde{q}^-) \frac{d}{dU_s} \varphi_s^{(0)} \quad (81)$$

The bulk chemical potentials $\mu_\alpha^{(0),\pm}$ are independent of U and using the global electroneutrality once more, we infer

$$\begin{aligned} \frac{d}{dU_s} \gamma^{(0)} &= - \sum_{\alpha \in \mathcal{M}^-} z_\alpha e_0 n_s^{(0)} \frac{d}{dU_s} \varphi^{(0),-} + \left(\sum_{\alpha \in \mathcal{M}^-} z_\alpha e_0 n_s^{(0)} + \tilde{q}^+ + \tilde{q}^- \right) \frac{d}{dU_s} \varphi^{(0),+} \\ &\quad - (\tilde{q}^+ + \tilde{q}^-) \frac{d}{dU_s} \varphi_s^{(0)} \\ &= \sum_{\alpha \in \mathcal{M}^-} z_\alpha e_0 n_s^{(0)} \frac{d}{dU_s} (\varphi^{(0),+} - \varphi^{(0),-}) + (\tilde{q}^+ + \tilde{q}^-) \frac{d}{dU_s} (\varphi^{(0),+} - \varphi_s^{(0)}) . \end{aligned} \quad (82)$$

With the definition (79) we get the result

$$\frac{d}{dU_s} \gamma^{(0)} = \sum_{\alpha \in \mathcal{M}^-} z_\alpha e_0 n_s^{(0)} + (\tilde{q}^+ + \tilde{q}^-) \frac{d}{dU_s} (\varphi^{(0),+} - \varphi_s^{(0)}) . \quad (83)$$

Boundary layer contributions. Because the leading order electrochemical potentials are constant in the layers, i.e.

$$\tilde{\mu}_\alpha^{(0)} = \mu_\alpha^{(0),\pm} - z_\alpha (\tilde{\varphi}^{(0)} - \varphi^{(0),\pm}) , \quad (84)$$

we see from Gibbs-Duhem relation that $\tilde{p}^{(0)}$ can be expressed as a function of $\tilde{\varphi}^{(0)} - \varphi^{(0),\pm}$. Then, from the momentum balance and Poisson equation we conclude

$$\tilde{p} - p^{ref} = (1 + \chi) \partial_z (\tilde{\varphi}^{(0)})^2. \quad (85)$$

Assuming monotonicity of $\tilde{\varphi}^{(0)}$, we get an differential equation for $\tilde{\varphi}^{(0)}$ of the form

$$\partial_z \tilde{\varphi}^{(0),\pm} = (1 + \chi) F^\pm(\tilde{\varphi}^{(0)} - \varphi^{(0),\pm}), \quad (86)$$

where the function F^\pm depends on the subdomain. Then, we can rewrite the boundary layer tension $\tilde{\gamma}^\pm$ as

$$\begin{aligned} \tilde{\gamma}^\pm &= \pm \int_0^{\pm\infty} (\partial_z \tilde{\varphi}^{(0)})^2 dz = \pm \int_{\tilde{\varphi}^{(0)}(0)}^{\tilde{\varphi}^{(0)}(\pm\infty)} F(\tilde{\varphi} - \varphi^{(0),\pm}) d\tilde{\varphi} \\ &= \pm \int_{\varphi_s^{(0)}}^{\varphi^{(0),\pm}} F^\pm(\tilde{\varphi} - \varphi^{(0),\pm}) d\tilde{\varphi} \end{aligned} \quad (87)$$

We define $U^\pm := \varphi^{(0),\pm} - \varphi_s^{(0)}$ and differentiate with respect to U^\pm to get

$$\begin{aligned} \frac{d}{dU^\pm} \tilde{\gamma}^\pm &= \pm \frac{d}{dU^\pm} \int_{-U^\pm}^0 F(\tilde{\varphi}) d\tilde{\varphi} \\ &= \mp F(-U^\pm) = \mp F(\varphi_s^{(0)}) = \mp (1 + \chi) \partial_z \tilde{\varphi}^{(0)}(0) \end{aligned} \quad (88)$$

We use the Poisson equation

$$\frac{d}{dU^\pm} \tilde{\gamma}^\pm = \pm \int_0^{\pm\infty} (1 + \chi) \partial_{zz} \tilde{\varphi}^{(0)} dz = \mp \int_0^{\pm\infty} \tilde{n}^F dz = -\tilde{q}^\pm. \quad (89)$$

Since $U = U^+ - U^-$ we have $U^\pm = U^\mp \pm U$ and $\frac{dU^-}{dU} = \frac{dU^+}{dU} - 1$ and deduce

$$\begin{aligned} \frac{d}{dU} (\tilde{\gamma}^+ + \tilde{\gamma}^-) &= \frac{dU^+}{dU} \frac{d}{dU^+} \tilde{\gamma}^+ + \frac{dU^-}{dU} \frac{d}{dU^-} \tilde{\gamma}^- \\ &= -\frac{dU^+}{dU} \tilde{q}^+ - \left(\frac{dU^+}{dU} - 1 \right) \tilde{q}^- = \tilde{q}^- - (\tilde{q}^+ + \tilde{q}^-) \frac{dU^+}{dU}. \end{aligned} \quad (90)$$

Putting together (83) and (90) we finally conclude

$$\frac{d}{dU} (\gamma + \tilde{\gamma}^+ + \tilde{\gamma}^-) = \sum_{\alpha \in \mathcal{M}^-} z_\alpha e_0 n_\alpha + \tilde{q}^-. \quad (91)$$

6 Electrocapillary of the metal-electrolyte interface

We consider now the interface between a liquid metal and a liquid electrolyte. First we state and explain the material functions for the metal, the electrolyte and the surface, where the chemical potentials are derived from material specific free energy densities of the respective phase[DGL16]. Based on this material functions we obtain representations of the boundary layer and surface charges and their contributions to the interfacial tension. In section 7 we apply our model to several Hg|aqueous electrolyte interfaces and compare our results to experimental data.

Notation. By convention the metal occupies the domain $\Omega^+ = \Omega^M$ and in the following we use the index M instead of + to denote quantities in the metal. According to this definition the electrolyte occupies the domain $\Omega^- = \Omega^E$ and we denote all electrolytic quantities with an index E. Further we omit the labeling with (0) and (1) of the leading and higher order and the tilde to distinguish between bulk and boundary layer.

We denote the potential difference in the leading order between metal-surface and electrolyte-surface as

$$U^M = \varphi^M - \varphi_s \quad \text{and} \quad U^E = \varphi - \varphi_s^E, \quad (92)$$

and the boundary layer charges as

$$Q_{BL}^M = \int_0^{+\infty} n^F dz \quad \text{and} \quad Q_{BL}^E = \int_{-\infty}^0 n^F dz. \quad (93)$$

6.1 Specific material model

The material functions given in this section are derived in detail in [DGL16]. We briefly summarize the results.

Metal The metal is modeled as mixture of metal ions denoted by M and valence electrons e^- , with respective number densities n_M and n_e . We consider the metal as an incompressible mixture, leading to the incompressibility constraint $n_M v_M^R = 1$, where v_M^R denotes the partial volume of a particle. For the chemical potentials we have

$$\mu_M = \psi_M^R + v_M^R p_M \quad \text{and} \quad \mu_e = \left(\frac{3}{8\pi} \right)^{2/3} \frac{h^2}{2m_e} n_e^{2/3}, \quad (94)$$

where μ_e is equal to the Fermi level of the considered metal. Note that p_M in (94) is the metal ion partial pressure which is related to the total material pressure p via

$$p = p_e + p_M \quad \text{and} \quad p_e = \frac{2}{5} \left(\frac{3}{8\pi} \right)^{2/3} \frac{h^2}{2m_e} n_e^{5/3}. \quad (95)$$

For the metallic boundary layer charge we obtain the representation

$$\hat{Q}_{BL}^M = -\text{sgn}(U^M) \sqrt{2\varepsilon_0(1 + \chi_M) e_0 n_M \left(U^M - \frac{2}{5} \frac{\mu_e^M}{e_0} \left(1 - \left(1 - \frac{e_0}{\mu_e^M} U^M \right)^{\frac{5}{2}} \right) \right)}. \quad (96)$$

Here, n_M denotes the density of metal (ions), μ_e^M the bulk chemical potential (or Fermi level) of the electrons, and U^M the potential drop within the metal boundary layer. For the boundary layer tension of the metal we obtain thus

$$\hat{\gamma}_{BL}^M = \int_0^{U^M} \sqrt{2\varepsilon_0(1 + \chi_M) e_0 n_M \left(U' - \frac{2}{5} \frac{\mu_e^M}{e_0} \left(1 - \left(1 - \frac{e_0}{\mu_e^M} U' \right)^{\frac{5}{2}} \right) \right)} dU', \quad (97)$$

which is a strictly positive for $U^M > 0$.

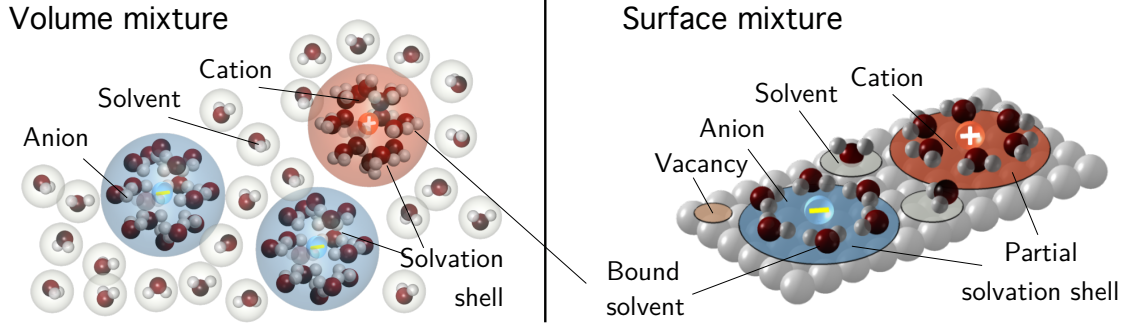


Figure 2: Sketch of the mixture constituents in the volume and on the surface. Anions and cations are particles which are composed from a center ion and a surrounding solvation shell of bounded and oriented solvent molecules. In addition there may be free solvent molecules and unoccupied sites on the surface.

Electrolyte. We consider the electrolyte as incompressible liquid mixture of constituents A_α , $\alpha = 0, 1, \dots, N$ with mole densities n_α . By convention A_0 denotes the solvent, while A_α , $\alpha = 1, \dots, N$ are ionic as well as undissociated species. For all constituents v_α^R is the partial volume and y_α the respective mole fraction. The incompressibility states

$$n \sum_{\alpha=0}^N v_\alpha^R y_\alpha = 1 \quad \text{with} \quad y_\alpha = \frac{n_\alpha}{n} \quad \text{and} \quad n = \sum_{\beta=0}^N n_\beta, \quad (98)$$

The chemical potentials of the electrolytic constituents in the incompressible limit is

$$\mu_\alpha = g_\alpha^R + v_\alpha^R (p - p^R) + k_B T \ln(y_\alpha), \quad \alpha = 0, 1, \dots, N, \quad (99)$$

with reference Gibbs free energy $g_\alpha^R = \psi_\alpha^R + v_\alpha^R p^R$. Note that due to the solvation effect several solvent molecules are bound in the solvation shell of the ionic constituents (cf. figure 2), which implies $v_0^R \ll v_\alpha^R$.

We obtain from the boundary layer equations (34) in the leading order an implicit equation system to determine the boundary layer charge

$$\hat{Q}_{\text{BL}}^E = -\text{sgn}(U^E) \sqrt{2\varepsilon_0(1+\chi)(p - p^E)} \quad \text{and} \quad g(p, U^E) = 0 \quad (100)$$

with

$$g(p, U^E) = \sum_{\alpha=0}^{N_E} y_\alpha^E e^{-\frac{z_\alpha e_0}{k_B T} U^E - \frac{v_\alpha^R}{k_B T} (p - p^E)} - 1. \quad (101)$$

Here y_α^E denotes the bulk mole fractions. Since $g(p, U^E) = 0$ is not explicitly solvable, $p = \hat{p}(U^E)$ denotes a local solution of (100)₂. We obtain thus the semi-explicit representation of the electrolytic boundary layer tension

$$\hat{\gamma}_{\text{BL}}^E := \int_0^{U^E} \sqrt{2\varepsilon_0(1+\chi)(\hat{p}(U') - p^E)} dU'. \quad (102)$$

which is positive for $U^E > 0$ and vanishes for $U^E = 0$.

Surface. The surface S is considered as mixture of the surface metal ions M , surface electrons e^- , and adsorbates A_α , $\alpha = 1, \dots, N_S - 2$, with respective surface number densities n_α . Since we consider the adsorption to occur on certain adsorption sites, we introduce surface vacancies via $n_V = \omega_M n_M - \sum_{\alpha=0}^{N_S} \omega_\alpha n_\alpha$. Here, ω_α denotes the adsorption site of constituent A_α . Quite similar to the volume phases we have an incompressibility constraint on the surface, stating $a_M^R n_M = 1$ where a_M^R is the partial area of surface metal ions. The chemical potential of the metal ions is

$$\mu_M = \psi_M^R + \omega_M k_B T \ln y_V - a_M^R \gamma \quad \text{with} \quad y_V = \frac{n_V}{\tilde{n}} \quad \text{and} \quad \tilde{n} = \sum_{\alpha=0}^{N_S-2} n_\alpha, \quad (103)$$

and of the adsorbates ($\alpha = 0, 1, \dots, N_S$)

$$\mu_\alpha = \psi_\alpha^R + k_B T \ln y_\alpha - \omega_\alpha k_B T \ln y_V. \quad (104)$$

We denote with γ the surface tension, y_V the surface fraction of vacancies and y_α the surface fraction of adsorbates. Note that we consider on the surface also a solvation effect, whereby each adsorbed ion binds κ_α solvent molecules.

For the electrons we consider the surface chemical potential to be a constant, i.e. $\mu_e = \mu_e^M$. Due to the adsorption equilibrium of the electrons on the metal surface we have the relation $U^M = \frac{1}{e_0} (\mu_e^M - \mu_e^s)$, where μ_e^M is the surface chemical potential of the electrons. Since μ_e^M as well as μ_e^s are constant, the potential drop $U^M = \varphi^M - \varphi$ is also constant.

The surface tension γ can be rewritten as $\gamma = \gamma^M - \gamma^E$ which has some beneficial properties. From the adsorption equilibrium of the metal ions we obtain a representation of γ^M , i.e.

$$\gamma^M = n_M^R \Delta g_M^A - z_M n_M^R e_0 U^M, \quad (105)$$

where n_M^R is the surface metal ion density, z_M the ionic charge number, and $\Delta g_M^A = \psi_M^R - g_M^R$ the constant adsorption energy of the metal ions. Form the surface equation (32a), we obtain for the surface mole fraction y_α of the vacancies and adsorbates A_α , $\alpha = 0, 1, \dots, N_S$ the expressions

$$y_V = e^{-\frac{a_M^R}{k_B T} \gamma^E} \quad \text{and} \quad y_\alpha = y_\alpha^E (y_0^E)^{(\kappa_\alpha - \kappa_\alpha)} e^{-\frac{\Delta g_\alpha^A}{k_B T} - \frac{z_\alpha e_0}{k_B T} U^E - \frac{a_\alpha^R}{k_B T} \gamma^E}. \quad (106)$$

We denote with Δg_α^A the (constant) adsorption energy and $\kappa_\alpha, \kappa_\alpha$ the respective solvation numbers of constituent A_α . Note that (106) implies $\gamma^E > 0$. Further the side condition $\sum_\alpha y_\alpha = 1$ yields

$$y_V(\gamma^E) + \sum_{\alpha=0}^{N_S} y_\alpha(\gamma^E, U^E) = 1, \quad (107)$$

which determines γ^E as a function of U^E , i.e. $\gamma^E = \hat{\gamma}^E(U^E)$.

Interface. We have thus a representation of the interfacial tension γ as function of the potential differences U^E and U^M ,

$$\gamma = \gamma^M - \gamma^E \quad \text{with} \quad \gamma^M = \gamma_s^M + \hat{\gamma}_{BL}^M = \hat{\gamma}^M(U^M) \quad \text{and} \quad \gamma^E = \gamma_s^E + \gamma_{BL}^E = \hat{\gamma}^E(U^E). \quad (108)$$

Note that $\gamma_{BL}^M > 0$ as well as $\gamma_{BL}^E > 0$ and $\gamma_s^E > 0$. The boundary layer in the electrolyte as well as the adsorption of electrolytic species can thus only lower the interfacial tension γ . Further, since $U^M = \text{const.}$, the contribution

$$\gamma^M = \gamma_s^M + \gamma_{BL}^M \quad (109)$$

is also constant. Instead of Δg_M^A as parameter of the model we can thus consider γ^M as parameter, which is essentially the surface tension of the liquid metal-vacuum or air interface.

An representation of the double layer charge Q is obtained in a similar manner. The surface charge n_s^F decomposes as $n_s^F = Q_s^E + Q_s^M$ with

$$Q_s^E = \frac{\sum_{\alpha=1}^{N_S} z_{\alpha} e_0 y_{\alpha}}{a_{V_s}^R y_V + \sum_{\alpha=0}^{N_S} a_{\alpha_s}^R y_{\alpha}} \quad (110)$$

and we obtain

$$Q = Q_{BL}^E + Q_s^E \quad (111)$$

with representations $Q_{BL}^E = \hat{Q}_{BL}^E(U^E)$ and $Q_s^E = \hat{Q}_s^E(U^E)$ [DGL16].

Applying a potential In an experiment the potential difference between the metal and some reference electrode is measured [DGL16]. Therefore we have to express the the potential difference between the metal and electrolyte $U = U^M + U^E$ as a function of the measured cell potential E between metal and reference electrode.

Let us consider a experimental setup with some reference electrode R, where the metal and the reference electrode are connected via cables C_1 and C_2 to a voltmeter V which measures a voltage E between its two identical, metallic plates V_1 and V_2 . The electrochemical cell, including measuring device and cables, may thus be written as



The measured cell potential E then corresponds to the surface potential difference between the two plates of the voltmeter, i.e.

$$E = \varphi_{V_1} - \varphi_{V_2}. \quad (113)$$

Due to the continuity of electrochemical potential $\mu_e - e_0\varphi$ of the electrons we have

$$E = U^E + U^R \quad \text{with} \quad U^R = -\frac{1}{e_0}(\mu_e^M - \mu_e^R) - U^{R,E} \quad (114)$$

where $U^{R,E} = \varphi_s^R - \varphi_s^E$ denotes the potential difference between bulk electrolyte and surface potential of the reference electrode. We follow the classical assumption of an *ideally non-polarizable (reference) electrode* [BRGA02], which states $U^{R,E} = \text{const.}$ Since μ_e^M is incorporated in U^R , we can consider U^R as model parameter instead of μ_e^M .

6.2 Lippmann equation

Due to the constant potential difference U^M and the simple relation (114) between the potential difference U^E and measured potential E the Lippmann equation (46) simplifies to

$$\frac{d\gamma}{dE} = Q. \quad (115)$$

This is the Lippmann equation which was very precisely confirmed by experimental measurements. However, in contrast to common (surface) thermodynamic approaches, which actually postulate the Lippmann equation (or a similar relationship), we derived it within the consistent framework of non-equilibrium thermodynamics.

A further derivative with respect to E of the Lippmann equation leads to an important relation, which is used to determine the differential capacity C from a interfacial tension measurement or vice versa,

$$\frac{d^2\gamma}{d^2E} = C. \quad (116)$$

6.3 Electrocapillarity maximum and potential of zero charge

The Lippmann equation (115) shows that the electrocapillarity maximum E^0 indeed corresponds to the potential of zero charge, i.e.

$$\left. \frac{d\gamma}{dE} \right|_{E=E^0} = 0 \quad \Leftrightarrow \quad Q|_{E=E^0} = 0 \quad (\text{with } \left. \frac{d^2\gamma_{\text{Int}}}{dE^2} \right|_{E^0} > 0). \quad (117)$$

However, since Q consists of two contributions, namely the boundary layer charge Q_{BL}^E and the adsorbate surface charge Q_s^E , the condition $Q = 0$ actually implies $Q_{\text{BL}}^E = -Q_s^E$, i.e. a balance between the adsorbate charge and the boundary layer charge. Note that the condition $Q = 0$ with $Q_{\text{BL}}^E = \hat{Q}_{\text{BL}}^E(E^0 - U^R)$ and $Q_s^E = \hat{Q}_s^E(E^0 - U^R)$ serves to determine E^0 . For a non-adsorbing salt holds $E^0 - U^R = 0$ [DGL16], while for an adsorbing salt E^0 depends parametrically on the salt concentration, the adsorption energies Δg_α^A , solvation numbers and so on.

7 Electrocapillarity of the Hg|aqueous electrolyte interface

In this section we discuss several representative examples in order to provide a model based understanding and interpretation of Fig. 1.

The following list provides a summary of the parameters arising in our model. A detailed discussion of the model parameters is given in [DGL16] and an upcoming work.

Electrolyte	Surface
Bulk particle densities $n_{\alpha}^E / \frac{\text{mol}}{\text{L}}$	Adsorption energy $\Delta g_{\alpha}^A / \text{eV}$
Solvent part. mol. volume $v_0^R = \frac{1}{55.5} / \frac{\text{L}}{\text{mol}}$	Metal part. mol. area $a_M^R = 5.09 \cdot 10^8 / \frac{\text{cm}^2}{\text{mol}}$
Temperature $T = 298 / \text{K}$	Reference potential $U^R = 0 / \text{V}$
Solvation number $\kappa_{\alpha} = z_{\alpha}^2 \cdot 45$	Surface Solvation number $\kappa_{\alpha,\beta}$
Ionic partial molar volumes $v_{\alpha}^R = (1 + \kappa_{\alpha})v_0^R$	Partial molar areas $a_{\alpha}^R = (1 + \kappa_{\alpha,\beta})a_M^R$
Dielectric susceptibility $\chi_E = 25$	Metal interf. tension $\gamma^M = 485.5 \cdot 10^{-3} / \frac{\text{N}}{\text{m}}$
Bulk pressure $p^E = 1 / \text{atm}$	

We discuss the following examples to investigate the impact of the respective parameter variation on the electrocapillarity curve:

- adsorption energy of solvent (Δg_0^A),
- volume solvation number (κ_{α}),
- multi-valent salts (z_{α}),
- dissociation degree (α_d),
- bulk concentration dependency (n_{α}^E),
- adsorption energies of ions (Δg_{α}^A),

The equation system in section 3.3 is used to compute numerically the interfacial tension with respect to the applied potential for the respective example.

7.1 Adsorption energy of the solvent

Consider the interface between Hg and some inert *gas* (interface 1) as well as between *water* and the same *gas* (interface 2). In the light of section XX, the interfacial tension of the two

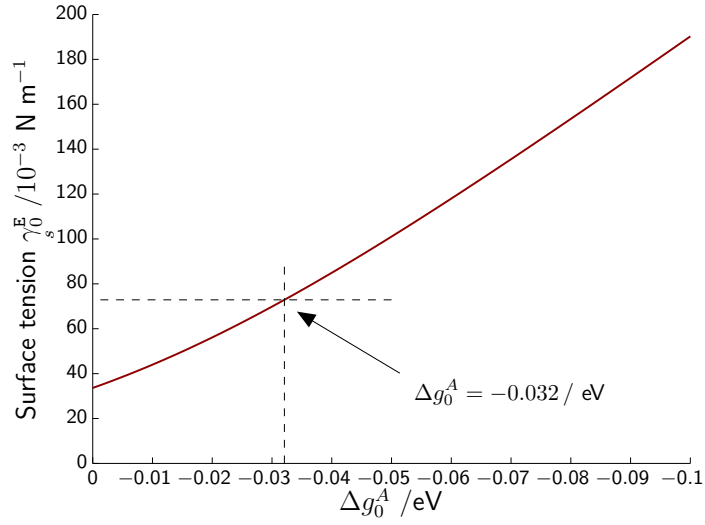


Figure 3: Plot of the relationship between Δg_0^A and the electrolyte tension γ^E according to the equation system (122), (123)₁ and (123)₂.

interfaces writes as

$$\gamma^{\text{Hg|gas}} = \gamma^{\text{Hg}} - \gamma^{\text{gas}} \quad \text{and} \quad \gamma^{\text{water|gas}} = \gamma^{\text{water}} - \gamma^{\text{gas}}. \quad (118)$$

Assuming that the γ^{gas} contribution remains equal for both interfaces, we obtain

$$\gamma^{\text{Hg|water}} = \gamma^{\text{Hg}} - \gamma^{\text{water}} = \gamma^{\text{Hg|gas}} - \gamma^{\text{water|gas}}, \quad (119)$$

which is the interfacial tension of a Hg|water interface. At 20°C we have the following values[Jas72]

$$\gamma^{\text{Hg|gas}} = 486.5 \cdot 10^{-3} / \frac{\text{N}}{\text{m}}, \quad \gamma^{\text{water|gas}} = 72.88 \cdot 10^{-3} / \frac{\text{N}}{\text{m}} \quad (120)$$

which gives

$$\gamma^{\text{Hg|water}} = 413.62 \cdot 10^{-3} / \frac{\text{N}}{\text{m}} \quad (121)$$

and is in well agreement to the measured data $\gamma_{\text{measured}}^{\text{Hg|water}} = 415 \cdot 10^{-3} / \frac{\text{N}}{\text{m}}$ [AG⁺67].

Next, assume for a moment that the adsorbate contributions of OH^- and H^+ are negligible i.e. $y_{\text{OH}^-} = y_{\text{H}^+} = 0$. Their contributions are separately discussed in section XX. Further, reconsider the representation (102) of γ_{BL}^E , which gives $\hat{\gamma}_{\text{BL}}^E(0) = 0$. For a pure Hg|water interface there is (at the potential of zero charge) only one contribution γ_0^E to the interfacial tension γ due to adsorbed solvent molecules. The surface tension contribution γ_0^E satisfies

$$y_0 = y_0^E e^{-\frac{\Delta g_0^A}{k_B T} - \frac{a_0^R}{k_B T} \gamma_0^E}. \quad (122)$$

together with

$$y_{V_s} = e^{-\frac{a_M^R}{k_B T} \gamma_0^E} \quad \text{and} \quad y_{V_s} + y_0 = 1. \quad (123)$$

The mercury ion surface density n_M^R is determined from $n_M = n_M^{\frac{2}{3}}$ with $n_M^R = 67.52 / \text{mol L}^{-1}$ according to the density of mercury. We obtain hence for the partial molar area of mercury $a_M^R = (n_M^R)^{-1} = 5.09 \cdot 10^8 / \frac{\text{cm}^2}{\text{mol}}$ and in a similar manner for the solvent $a_0^R = 5.08 \cdot 10^8 / \frac{\text{cm}^2}{\text{mol}}$. Hence the number of surface sites of water is $\omega_0 = 1$. The interfacial tension contribution γ_0^E is thus exclusively determined by Δg_0^A , i.e. $\gamma_0^E = f(\Delta g_0^A)$ (Fig. XX). We can choose Δg_0^A such that $\gamma^E = 72.88 \cdot 10^{-3} / \text{N m}^{-1}$, which essentially determines the model parameter $\Delta g_0^A = -0.032 / \text{eV}$ from an *independent* experiment, i.e. water|gas interface tension measurements. This value is used for all upcoming examples of aqueous electrolyte mixtures.

7.2 Volume solvation number

Consider now some non-adsorbing salt AC which completely dissociates in anions A^- and cations C^+ . According to our model, each ion A_α binds κ_α solvent molecules in its solvation shell.

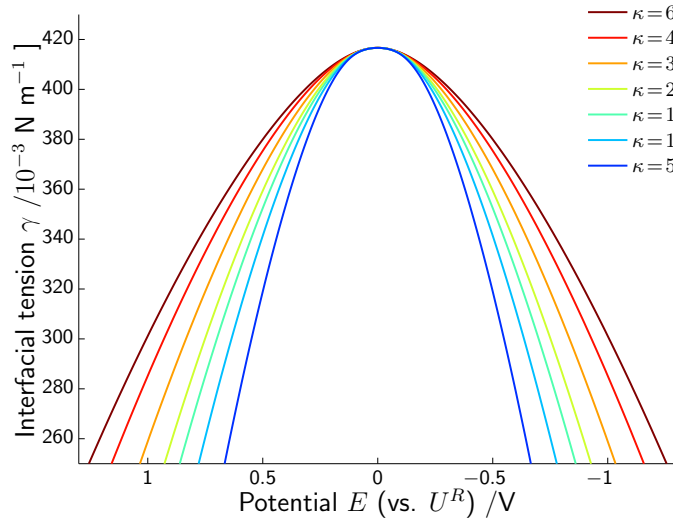


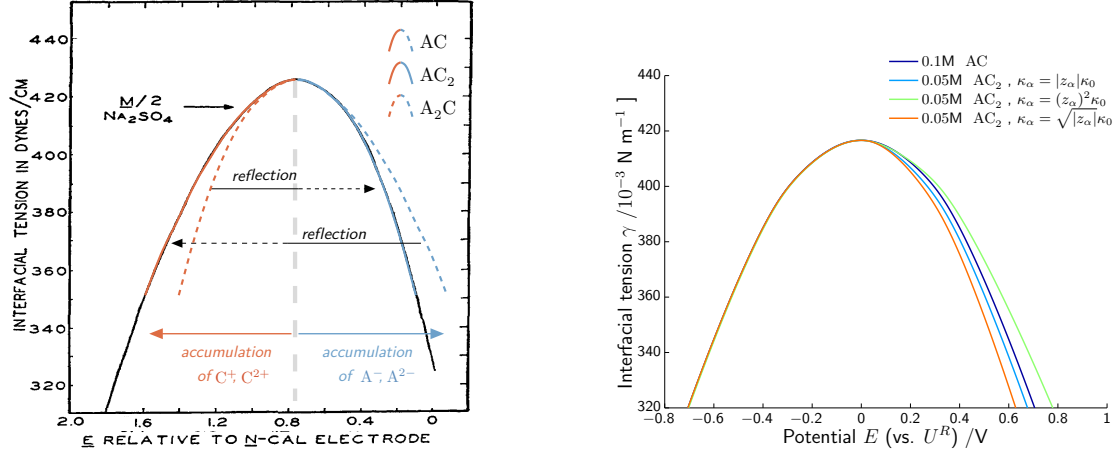
Figure 4: Dependency of the interfacial tension γ on the solvation number κ_α for a completely dissociated salt AC.

This is a crucial parameter for the interfacial tension value γ , or more precise, for the contribution γ_{BL}^E of the electrolytic boundary layer (see Fig. XX). In our validation study in the Ag|aqueous electrolyte interface we determined $\kappa_\alpha = \kappa_0 \approx 45$ for mono-valent ions. Since the solvation effect arises from the microscopic interaction between the central ion and some polar solvent

molecules, it is expectably that the solvation number depends κ_α depends on the charge number z_α . Several relationships are imaginable, e.g. $\kappa_\alpha = |z_\alpha| \cdot \kappa_0$, $\kappa_\alpha = z_\alpha^2 \cdot \kappa_0$ or $\kappa_\alpha = \sqrt{|z_\alpha|} \cdot \kappa_0$, which are discussed in the next section on measurements of Na_2SO_4 .

7.3 Charge number and dissociation degree

The charge numbers of the ionic compounds of some multi-valent salt also effects the electrocapillarity curve.



(a) Interfacial tension measurement of the mercury| $0.05M \text{Na}_2\text{SO}_4$ interface (Fig. 20 from [Gra47], Data by Gouy[Gou06a, Gou06a, Gou06b])

(b) Computation of the interfacial tension for multi-valent salts with various models of κ_α .

Figure 5: Comparison of the interfacial tension of multi-valent, completely dissociated salts.

Figure 5 displays the influence of multi-valent salts on the interfacial tension, where Na_2SO_4 is considered as experimental example. In figure 5a we reflected the right and left branch of the electrocapillarity curve on the dashed line, i.e. at the potential of zero charge. This clearly shows that the interfacial tension is not symmetric w.r.t. to potential of zero charge. A comparison of this measurement to our computations of multi-valent salts (Fig. 5b) explains this effect quite well if one assumes complete dissociation of Na_2SO_4 in Na^+ and SO_4^{2-} . The best result is obtained for $\kappa_\alpha = \sqrt{|z_\alpha|} \cdot \kappa_0$ which is used in the further discussion. A detailed investigation of the relationship between the solvation and charge number as well as a microscopic interpretation of the relation

$$\kappa_\alpha = \sqrt{|z_\alpha|} \cdot \kappa_0 \quad (124)$$

will be given separately, since it is not scope of this work. It seems, however, quite reasonable that the solvation number increases with the charge number and that this relation is not necessarily linear.

When considering multi-valent ions, it is crucial to have detailed knowledge on the dissociation degree of the corresponding salt. We find in the introductory electrocapillarity curves for example

$\text{Ca}(\text{NO}_3)_2$, for which one could naively assume complete dissociation $\text{Ca}(\text{NO}_3)_2 \rightleftharpoons \text{Ca}^{2+} + 2\text{NO}_3^-$. However, calcium nitrate does not necessarily dissociate in 2-valent calcium ions. Calcium does react with hydroxide to form (dissolved) CaOH^+ , i.e. $\text{Ca}^{2+} + \text{OH}^- \rightleftharpoons \text{CaOH}^+$, which changes the pH value of the solution. Additionally, the first dissociation step $\text{Ca}(\text{NO}_3)_2 \rightleftharpoons \text{CaNO}_3^+ + \text{NO}_3^-$ could be dominant in the dissolution of $\text{Ca}(\text{NO}_3)_2$, forming thus *mainly* mono-valent cations CaNO_3^+ and CaOH^+ .

In fact, electrocapillarity measurements provide some fascinating insights on the dissociation degree of a multi-valent salt! If the electrocapillarity of **is** symmetric w.r.t. the potential of zero charge, the charge numbers of the ionic species in solution are necessarily equal. For $\text{Ca}(\text{NO}_3)_2$ we find a symmetric behavior, which suggest the dissociation of $\text{Ca}(\text{NO}_3)_2 \rightleftharpoons \text{CaNO}_3^+ + \text{NO}_3^-$ instead of a (complete) dissociation $\text{Ca}(\text{NO}_3)_2 \rightleftharpoons \text{Ca}^{2+} + 2\text{NO}_3^-$.

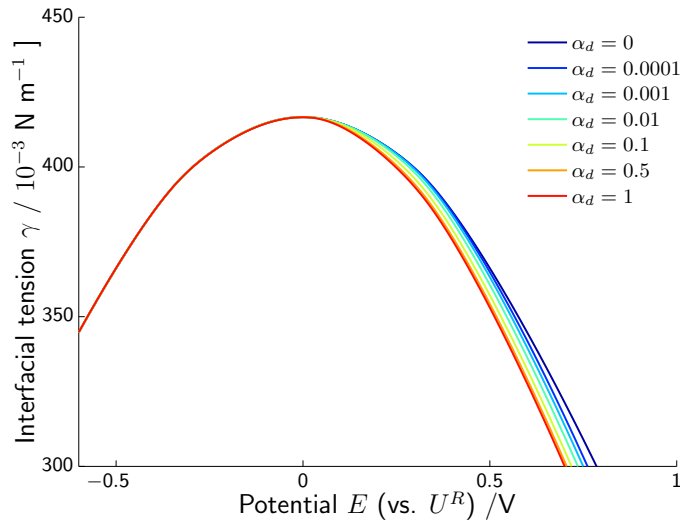
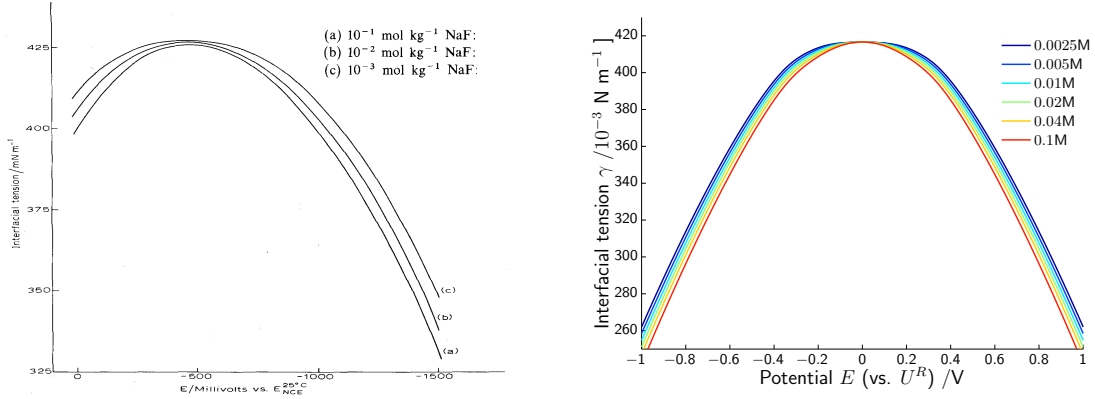


Figure 6: Impact of the dissociation degree on the electrocapillarity curve.

Exemplarily consider AC_2 which is assumed to dissociate completely into species A^{2-} , AC^- , C^+ . However, there is a remaining dissociation degree $\alpha_d \in [0, 1]$ of the reaction $\text{AC}^- \rightleftharpoons \text{A}^{2-} + \text{C}^+$, with $\alpha_d = 1$ meaning complete dissociation of AC_2 in A^{2-} and C^+ , while $\alpha_d = 0$ means complete dissociation in AC^- and C^+ . Figure 6 displays the impact of the dissociation degree on the electrocapillarity curve. Expectably, the left branch remains unchanged since the bulk density and valance number of the cations remains unchanged.

7.4 Salt concentration

Yet we have investigated the electrocapillarity curve for a fixed (equivalent) concentration of 0.1M. It is, however, well known that the interfacial tension is dependent on the electrolyte concentration[Gou06a, Gou06b, Gou03]. Fig. 7 displays numerical solutions of our model for the concentration range 0.0025 – 0.1M of a completely dissociated, non-adsorbing salt AC.



(a) Electrocapillarity curves for NaF solutions (Fig. 2 of [CDJH74]).

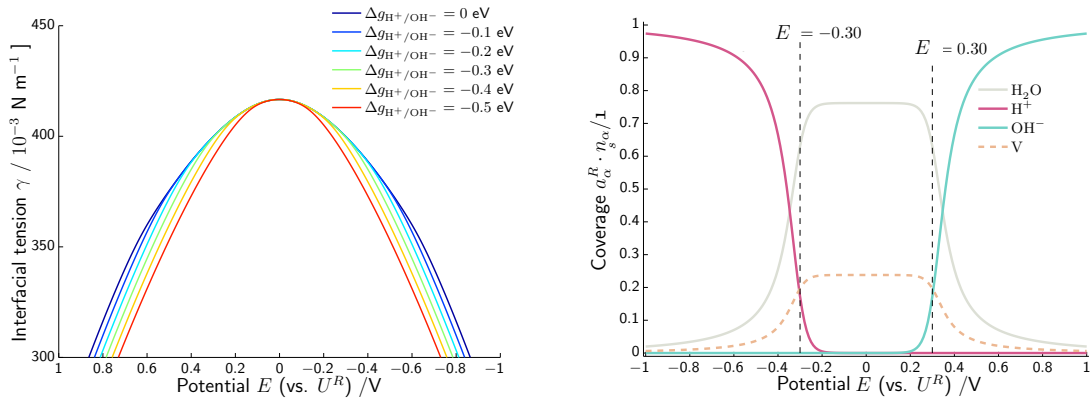
(b) Parameter study of the salt concentration for a mono-valent salt AC.

Figure 7: Salt concentration dependency of the electrocapillarity curve.

7.5 Adsorption energies

Several adsorption energies arise in our model for some arbitrary electrolytic mixture. These are namely

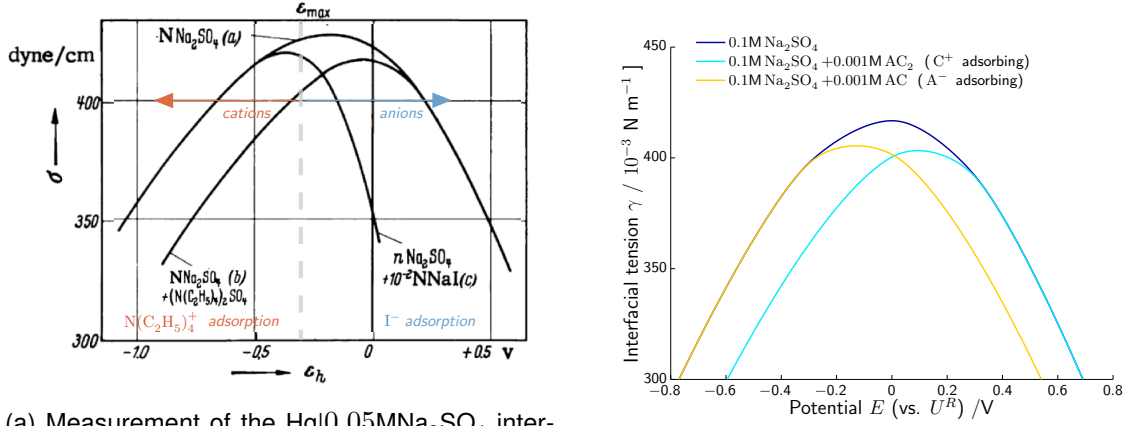
- the adsorption energies $\Delta g_{\text{OH}^-}^A$ and $\Delta g_{\text{H}^+}^A$ of protons and hydroxide ions,
- the adsorption energies of anions and the cation,
- and the adsorption energies of undissociated ionic compounds or other uncharged additives.



(a) Parameter study of $\Delta g_{\text{OH}^-}^A = \Delta g_{\text{H}^+}^A$ and its impact on the electrocapillarity curve for a 0.1M non-adsorbing salt AC.

(b) Coverage of the mercury surface for $\Delta g_{\text{OH}^-}^A = \Delta g_{\text{H}^+}^A = -0.3 \text{ eV}$. Even though H^+ and OH^- have relatively small bulk concentrations, i.e. $10^{-7} \text{ mol L}^{-1}$, adsorption starts at about $\pm 0.3 \text{ V}$.

Figure 8: Investigations on the adsorption of H^+ and OH^- on the mercury surface.



(a) Measurement of the Hg|0.05MNa₂SO₄ interface (a) and with cation adsorbing additives (b) and anion adsorbing additives (c) (Fig. 36 of [VBHT67], Data by Gouy [Gou06a, Gou06a, Gou06b]).

(b) Computation of mercury|0.05MNa₂SO₄ (blue) with cation (yellow) and anion (cyan) adsorbing additives.

Figure 9: Comparison of the interfacial tension for adsorbing cation and anion additives.

Adsorption of protons and hydroxide ions We investigate first the adsorption energies of $\Delta g_{\text{OH}^-}^A$ and $\Delta g_{\text{H}^+}^A$. We assume that for pure water the potential of zero charge (for $U^R = 0$) is equal to zero, which implies that if OH⁻ and H⁺ adsorb on the metal surface, their surface concentrations are equal and thus necessarily $\Delta g_{\text{OH}^-}^A = \Delta g_{\text{H}^+}^A$. Figure 8a displays the impact of the OH⁻ and H⁺ adsorption on the electrocapillarity. A detailed chemical based discussion on the adsorption energies of protons and hydroxide ions is not subject of this work. We rather show the impact of H⁺ and OH⁻ adsorption on the electrocapillarity. Since one would expect a slight adsorption of H⁺ and OH⁻ on the mercury surface, we choose $\Delta g_{\text{OH}^-}^A \approx -0.3\text{eV}$ which ensures the adsorption in a reasonable potential range (see the coverage computation in Fig. 8b). All computations throughout this work were performed with the value $\Delta g_{\text{OH}^-}^A = \Delta g_{\text{H}^+}^A = -0.3\text{eV}$. Note, however, that this is a metal specific quantity and could be very different for other materials.

Adsorption of ions Next we discuss the adsorption of anions and cations. Specific adsorption of anions shifts the potential of zero charge in negative direction, while for cations it shifts positive. Fig. 9 shows a comparison between the data of K. Vetter[VBHT67] and a computation of our model.

The computation of Fig. 9b is based on the parameters $\Delta g_{\text{C}^+}^A = -0.65/\text{eV}$ (while $\Delta g_{\text{A}^{2-}}^A = 1\text{eV}$, no anion adsorption) for the yellow curve and $\Delta g_{\text{A}^-}^A = -0.65/\text{eV}$ (while $\Delta g_{\text{C}^+}^A = 1\text{eV}$, no cation adsorption) for the cyan curve.

Comparing our results with the measurements of K. Vetter (Fig. 9a) shows (i) a quite good qualitative and quantitative agreement. The unsymmetric behavior w.r.t. the potential of zero charge originates from the multi-valent anions SO₄²⁻ (c.f. section 7.3).

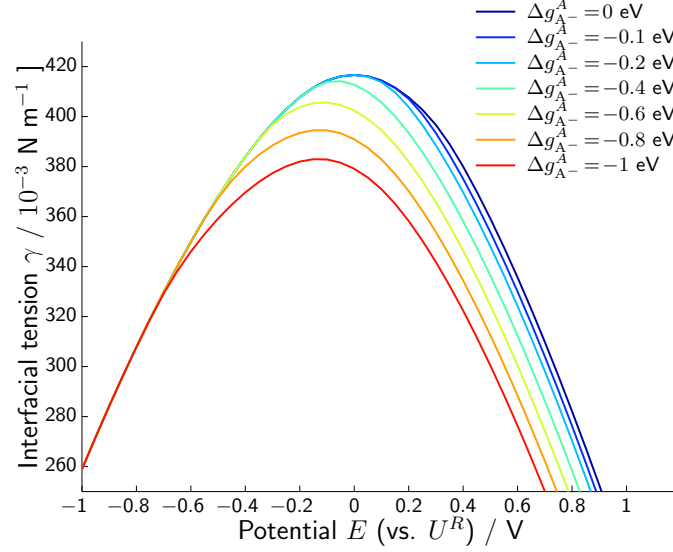


Figure 10: Parameter study of the anion adsorption energy Δg_{α}^A and its impact on the electrocapillarity curve.

We provide finally a parameter study of the adsorption energy Δg_{α}^A of the mono-valent anion of a 0.1M AC mixture. This is considered as representative example for salts having the same cation but different anions, e.g. KCl, KI, KOH. Expectably, if we decrease the adsorption energy Δg_{α}^A , adsorption occurs *earlier* w.r.t. the potential of zero charge of a non-adsorbing salt. Additionally we clearly find the contribution of the ionic adsorbates on the value of the electrocapillary maximum. With respect to the introductory example we choose

$$\Delta g_{\text{Cl}^-} = -0.4\text{eV}, \Delta g_{\text{Br}^-} = -0.5\text{eV}, \Delta g_{\text{I}^-} = -0.6\text{eV} \quad (125)$$

while the anions SO_4^{2-} and NO_3^- do not adsorb (i.e. $\Delta g_{\alpha}^A > 1\text{eV}$). We already showed that the surface solvation is dependent on the specific constituent [DGL16], and we employ here

$$\kappa_{\text{Cl}^-} = 20, \kappa_{\text{Br}^-} = 15, \kappa_{\text{I}^-} = 10. \quad (126)$$

Origin of the various surface solvation numbers is probably the partial charge transfer [SG14], which is, however, discussed in an independent work. Together with the parameters given in the overview of 7, these parameters served to compute the electrocapillarity curves of Fig. 1b.

8 Summary

Within this work we derive in detail the thermodynamic relations which explain the electrocapillarity effect. Rather than postulating the Lippmann-equation, we derive it based on non-equilibrium thermodynamics and matched asymptotic methods. This procedure was performed for some general interface between two charged phases. For the specific example of the liquid metal-aqueous electrolyte interface we provide explicit material functions which allow for the computation of the interfacial tension. Our model shows a remarkable qualitative and quantitative agreement to

experimental data and it should be considered as the very basis of a model based understanding of electrocapillarity curves. Detailed investigations on the various equilibrium parameters arising in our model were carried out in order to provide insight on the respective dependency.

A Appendix

A.1 Rescaling to dimensionless variables

$\mathbf{x} \rightarrow L^{ref} \mathbf{x}$	$m_\alpha \rightarrow m^{ref} m_\alpha$	$n_\alpha \rightarrow n^{ref} n_\alpha$
$\varphi \rightarrow \frac{kT}{e_0} \varphi$	$\mathbf{b} \rightarrow \frac{kT}{m^{ref} L^{ref}} \lambda \mathbf{b}$	
$\rho\psi \rightarrow n^{ref} kT \rho\psi$	$\mu_\alpha \rightarrow kT \mu_\alpha$	
$\Sigma \rightarrow n^{ref} kT \Sigma$	$p \rightarrow n^{ref} kT p$	

Table 1: Substitution in the bulk regions Ω^\pm .

$k_M \rightarrow \frac{1}{L^{ref}} k_M$	$n_\alpha \rightarrow n_s^{ref} n_\alpha$	$\mathbf{b} \rightarrow \frac{kT}{m^{ref} L^{ref}} \lambda \mathbf{b}$
$\rho\psi \rightarrow kT n_s^{ref} \rho\psi$	$\mu_\alpha \rightarrow kT \mu_\alpha$	$\gamma \rightarrow n_s^{ref} kT \gamma$

Table 2: Substitution on the interface S .

Discussion of the dimensionless numbers. We assume a number density n^{ref} which corresponds to a 0.1 molar aqueous solution. The characteristic number densities for the surfaces n_s^{ref} are given by typical spacing of the crystal lattice of a metal.

$$n^{ref} = 6.022 \cdot 10^{25} \text{ m}^{-3}, \quad n_s^{ref} = 7.3 \cdot 10^{18} \text{ m}^{-2}. \quad (127)$$

Given a characteristic length of the macroscopic system

$$L^{ref} = 10^{-2} \text{ m} \quad (128)$$

At room temperature $T = 298.15 \text{ K}$ and with the standard gravity of Earth $g = 9.81 \text{ ms}^{-2}$, we get the dimensionless numbers

$$\lambda \approx 1.54 \cdot 10^{-8}, \quad \lambda \delta \approx 1.21 \cdot 10^{-5}, \quad \lambda |\mathbf{b}| \approx 2.38 \cdot 10^{-8}. \quad (129)$$

References

[AG⁺67] A. W. Adamson, A. P. Gast, et al. *Physical chemistry of surfaces*. Interscience New York, 1967.

- [BD14] D. Bothe and W. Dreyer. Continuum thermodynamics of chemically reacting fluid mixtures. *Acta Mech.*, pages 1–49, 2014.
- [Bed86] D. Bedeaux. Nonequilibrium thermodynamics and statistical physics of surfaces. In Prigogine Ilya and S. A. Rice, editors, *Advances in Chemical Physics*, volume 64, pages 47–109. John Wiley Sons, Inc., 1986.
- [BF01] A.J. Bard and L.R. Faulkner. *Electrochemical methods: fundamentals and applications*. Wiley New York, 2 edition, 2001.
- [BRGA02] J.O’M. Bockris, A.K.N. Reddy, and M.E. Gamboa-Aldeco. *Modern Electrochemistry*, volume 2A: Fundamentals of Electrodics. Kluwer Academic Publishers, 2nd edition, 2002.
- [CDJH74] N.H. Cuong, C.V. D’Alkaine, A. Jenard, and H.D. Hurwitz. The surface phase at the ideal polarized mercury electrode: 2. coulostatic measurements at the Hg electrode in dilute NaF aqueous solutions at various temperatures. *J. Electroanal. Chem.*, 51(2):377 – 393, 1974.
- [CF88] G. Caginalp and P. Fife. Dynamics of layered interfaces arising from phase boundaries. *SIAM J. Appl. Math.*, 48(3):506–518, 1988.
- [DGK14] W. Dreyer, J. Giesselmann, and C. Kraus. A compressible mixture model with phase transition. *Physica D*, 273–274:1–13, 2014.
- [DGL14] W. Dreyer, C. Gohlke, and M. Landstorfer. A mixture theory of electrolytes containing solvation effects. *Electrochem. Commun.*, 43:75–78, 2014.
- [DGL16] W. Dreyer, C. Gohlke, and M. Landstorfer. Theory and structure of the metal-electrolyte interface incorporating adsorption and solvation effects. *Electrochimica Acta*, pages –, 2016.
- [DGM15] W. Dreyer, C. Gohlke, and R. Müller. Modeling of electrochemical double layers in thermodynamic non-equilibrium. *Phys. Chem. Chem. Phys.*, 17:27176–27194, 2015.
- [dM84] S. R. deGroot and P. Mazur. *Non-equilibrium Thermodynamics*. Courier Corporation, 1984.
- [Fru28] A. Frumkin. *Die Elektrokapillarkurve*, chapter 7, pages 235–275. Ergebnisse der Exakten Naturwissenschaften. Springer Berlin Heidelberg, Berlin, Heidelberg, 1928.
- [Gou03] L. G. Gouy. Sur la fonction électrocapillaire. *Ann. chim. phys.*, 29:145–241, 1903.
- [Gou06a] L. G. Gouy. Sur la fonction électrocapillaire. *Ann. chim. phys.*, 8:291–363, 1906.
- [Gou06b] L. G. Gouy. Sur la fonction électrocapillaire. *Ann. chim. phys.*, 9:75–139, 1906.
- [Gou10] L. G. Gouy. Sur la constitution de la charge électrique à la surface d’un électrolyte. *Journal de Physique Théorique et Appliquée*, 9(4):457–468, 1910.

- [Gra47] D. C. Grahame. The electrical double layer and the theory of electrocapillarity. *Chem. Rev.*, 41(3):441–501, 1947.
- [Guh15] C. Guhlke. *Theorie der elektrochemischen Grenzfläche*. PhD thesis, TU-Berlin, 2015.
- [Jas72] J. J. Jasper. The surface tension of pure liquid compounds. *Journal of Physical and Chemical Reference Data*, 1(4):841–1010, 1972.
- [Lip73] G. Lippmann. Beziehungen zwischen den capillaren und elektrischen Erscheinungen. *Ann. Phys.*, 225(8):546–561, 1873.
- [Lip75] G. Lippmann. *Relations entre les phénomènes électriques et capillaires*. PhD thesis, 1875.
- [MR59] J. Meixner and H. G. Reik. *Thermodynamik der irreversiblen Prozesse*, volume 3, pages 413–523. Springer, Berlin, 1959.
- [Mül85] I. Müller. *Thermodynamics, Interaction of Mechanics and Mathematics Series*. Pitman Advanced Publishing Program, Boston, 1985.
- [NTA04] J. Newman and K.E. Thomas-Alyea. *Electrochemical Systems*. Wiley, 2004.
- [Peg89] R.L. Pego. Front migration in the nonlinear Cahn-Hilliard equation. *Proc. R. Soc. Lond. A*, 422(1863):261–278, 1989.
- [SG14] W. Schmickler and R. Guidelli. The partial charge transfer. *Electrochim. Acta*, 127:489 – 505, 2014.
- [VBHT67] K.J. Vetter, S. Bruckenstein, B. Howard, and S. Technica. *Electrochemical kinetics*. Academic Press, 1967.